Modelling of shear stiffness of unsaturated fine grained soils at very small strains

K. S. Wong[a,*], D. Mašín[a] and C. W. W. Ng[b]

[a]Department of Engineering Geology, Institute of Hydrogeology, Engineering Geology and Applied Geophysics, Faculty of Science, Charles University in Prague, Prague, Czech Republic

[b]Department of Civil and Environmental Engineering, The Hong Kong University of Science and Technology, Clear Water Bay, Kowloon, Hong Kong

[*]Corresponding author: K. S. Wong

Researcher Associate, Department of Engineering Geology, Institute of Hydrogeology, Engineering Geology and Applied Geophysics, Faculty of Science, Charles University in Prague, Prague, Czech Republic

E-mail: wks46300wks@gmail.com

Co-author: D. Mašín

Associate Professor, Department of Engineering Geology, Institute of Hydrogeology, Engineering Geology and Applied Geophysics, Faculty of Science, Charles University in Prague, Prague, Czech Republic

E-mail: masin@natur.cuni.cz

Co-author: C.W.W.Ng

Chair professor, Department of Civil and Environmental Engineering, The Hong Kong University of Science and Technology, Clear Water Bay, Kowloon, Hong Kong.

E-mail: cecwwng@ust.hk

Abstract: The shear modulus at very small strains (less than 0.001%) is an important parameter in the design of geotechnical structures subjected to static and cyclic loadings. Although numerous soil models are available for predicting shear modulus of saturated and dry soils, only a few ones can predict shear stiffness at very small strains of unsaturated soils correctly. In this study, a few unsaturated soil models are evaluated critically and compared with a newly developed model. This newly proposed model is verified by using measured shear modulus at very small strains for three different low plasticity fine grained soils available in the literature. It is found that this new model can predict shear modulus at very small strain resulting from an increase and a decrease in mean net stress at constant matric suction for low plasticity fine grained soils. Moreover, this model is able to give a reasonably good prediction on shear stiffness at very small strain during wetting of a collapsible unsaturated soil. In addition, the newly proposed model is illustrated to capture a consistent trend with experimental data of shear stiffness at very small strain for non-collapsible soils obtained during drying-wetting cycles. This evaluation revealed that the newly proposed model has better predictive capabilities than some earlier formulations of the same simplicity. In addition, the proposed model with fewer parameters has similar predictive capability as compared with a more complex model.

Keywords: Shear modulus; very small strains; low plasticity; fine grained soil

1. Introduction

The shear modulus at very small strains (0.001% or less), G_o is a key parameter in the design of geotechnical structures subjected to static and cyclic loadings. Although numerous researches have been conducted on the measurement of shear modulus at very small strain and empirical formulations were proposed and verified for saturated and dry soils, high quality experimental data on G_o for unsaturated soils have only been available recently (Biglari et al., 2012; Mancuso et al., 2002; Ng and Xu, 2012; Ng et al., 2009; Ng and Yung, 2008; Vassallo et al., 2007a).

A few models have been proposed to predict shear modulus at very small strains for unsaturated soils. Some of them are simple semi-empirical formulations (Khosravi and McCartney, 2009; Leong et al., 2006; Ng and Yung, 2008; Sawangsuriya et al., 2009) while others involve more complex formulation with large number of variables (Biglari et al., 2011; Khosravi and McCartney, 2012; Vassallo et al., 2007). Most of the existing models can predict shear modulus at very small strains due to an increase of mean net stress at constant suction or due to an increase of suction at constant mean net stress. Some of the existing models also include effects of stress history. However, most of the models cannot predict shear modulus for wetting-induced collapsible soil and the effects of suction history on shear stiffness are not included. This study is carried out to propose a new formulation, which is simple but capable to consider the effects of suction history and can be used to predict shear modulus for wetting-induced collapsible soil. In addition, the new formulation is consistent with the definition of hydro-mechanical models for unsaturated soils by Mašín and Khalili (2008) and Mašín (2010). We aim to use it as a small-strain component of the newly developed hydro-mechanical hypoplastic model for variably saturated soils. The model will be based on the explicit hypoplastic formulation by Mašín (2013) and it will incorporate small strain stiffness anisotropy as proposed by Mašín and Rott (2013).

Three different low plasticity fine grained soils available in the literature are used to evaluate the newly proposed formulation.

2. Existing models for small strain stiffness of unsaturated soils

In general, formulations used in the existing models in predicting shear modulus at very small strain are of the following form:

$$G_o = \alpha\sigma^n \quad (1)$$

where α and n are constants and σ is a stress state variable. The models can be divided into two primary groups depending on the stress variables used in the model. The first primary group adopts the following form:

$$G_o = \alpha f(p - u_a) g_1(s) + \beta g_2(s) \quad (2)$$

where mean net stress, $(p - u_a)$ and matric suction, $s = (u_a - u_w)$ are used in the formulation. p, u_a and u_w are total mean stress, pore air and pore water pressures respectively. The first primary group can further be sub-divided into two categories depending on whether $\beta = 0$ or $\beta > 0$. Mancuso, Vassallo & d'Onofrio (MVD) model proposed by Mancuso et al. (2002), Leong, Cahyadi & Rahardjo (LCR) model suggested by Leong et al. (2006) and Ng & Yung (NY) model proposed by Ng and Yung (2008) are under category with $\beta = 0$. All the models are summarised in Table 1.

In the MVD model, net mean stress and matric suction where the transition between saturated and unsaturated state occurs, s_e are used. A, m and n are dimensionless parameters. For suction less than air entry value, they assumed that bulk-water effects dominate the behaviour of soil and the formulation for a saturated soil was adopted. For suction larger than the air entry value, they assumed that the shear modulus increases with suction and approaches a threshold value, at which soil behaviour is dominated by menisci water. A suction function, h(s) with dimensionless parameters, β_s and r_s is introduced for suction larger

than s_e. The threshold value of shear modulus is equal to $r_s G_{ose}$ where G_{ose} is G_o at s_e. Effects of stress history are included in the model through an overconsolidation ratio, OCR. Biglari et al. (2011) found that MVD model is not suitable in predicting shear modulus at very small strain for collapsible, normally consolidated unsaturated soil. The hardening induced by plastic volume reduction during wetting of collapsible unsaturated soil is not considered in the model.

In the LCR model, mean net stress and matric suction are normalised by atmospheric pressure, p_a = 100 kPa and k is a dimensionless parameters. The model was found to provide a good prediction for clayey sand at different net mean stresses and suctions.

NY model has the following equation for shear modulus at very small strain,

$$G_o = A\rho e^m \left[\left(\frac{p-u_a}{p_r}\right)^n\right]\left[1+\frac{s}{p_r}\right]^k \quad (3)$$

where p_r is a reference pressure and bulk density, $\rho = (G_s+S_r e)/(1+e)\rho_w$. G_s, S_r and e are respectively specific gravity, degree of saturation and void ratio. ρ_w is density of water. A void ratio function, ρe^m is included unlike in the MVD and LCR models. The void ratio function can be used to model the effects of stress history instead of using an overconsoliation ratio. NY model have been chosen to represent this category in the subsequent evaluation in view of the similarity of this model with the newly proposed model.

Vassallo, Mancuso & Vinale (VMV) model by Vassallo et al. (2007b) and Sawangsuriya, Edil & Bosscher first (SEB1) model by Sawangsuriya et al. (2009) are under category with $\beta > 0$. VMV model as summarised in Table 1 is based on Barcelona Basic Model (Alonso et al., 1990) framework. In the model, a void ratio function,

$$f_1(e) = \frac{(2.973-e)^2}{1+e} \quad (4)$$

is used. Effects of stress history are catered through an overconsolidation ratio, OCR = $(p - u_a)_o/(p - u_a)$ with $(p - u_a)_o$ at loading collapse (LC) curve at current suction. They found that the void ratio function $f_1(e)$ alone is not capable to cater the stress history effects. Effects of suction history are considered using function $H(s_o/s)$ where s_o is the maximum suction experienced by the unsaturated soil and β and r are two dimensionless parameters. They assumed that yielding on LC does not cause a significant shift of the suction increase (SI) surface in Barcelona Basic Model. Unfortunately, the publication does not contain an explicit function of $g_2(s)$.

SEB1 model has the following equation for shear modulus at very small strain,

$$G_o = Af_2(e)(p - u_a)^n + CS_r s \tag{5}$$

in which

$$f_2(e) = \frac{1}{0.3 + 0.7e^2} \tag{6}$$

where C is a dimensionless parameter. They adopted a different void ratio function than the VMW model and the effects of stress history are not included. SEB1 model has an explicitly defined function to cater effects of suction. As the VMV model does not contain an explicit function for suction effects, SEB1 model is selected to represent this category in the subsequent evaluation.

The second of the primary groups of models adopts the following form:-

$$G_o = \alpha f[(p - u_a), s] \tag{7}$$

There are four models in this group, namely Sawangsuriya, Edil & Bosscher second (SEB2) model proposed by Sawangsuriya et al. (2009); Khosravi & McCartney first (KM1) model suggested by Khosravi and McCartney (2009); Biglari, Mancuso, d'Onofrio, Jafari & Shafiee (BMDJS) model proposed by Biglari et al. (2011) and Khosravi & McCartney second (KM2)

model presented by Khosravi and McCartney (2012). All the models are summarised in Table 2.

SEB2 model adopts an isotropic average soil skeleton stress,

$$p' = (p - u_a) + \chi s \tag{8}$$

where $\chi = S_r$. KM1 model has isotropic average soil skeleton stress different from that in SEB2 model. It is derived based on suction stress characteristic curve concept (Lu and Likos, 2006) and the corresponding suction stress is obtained from shear strength equation proposed by Kayadelen et al. (2007). Suction at air entry or air expulsion is adopted in KM1 model while degree of saturation is used in SEB2 model.

BMDJS model is based on a framework suggested by Gallipoli et al. (2003). The formulation is as follows,

$$G_o = A p_a^{1-n} f_1(e) OCR_{p'}^{m} (p')^n h(S_r) \tag{9}$$

in which isotropic average soil skeleton stress from Equation 8 is adopted, function

$$h(S_r) = 1 - a'[1 - \exp(b'\zeta)] \tag{10}$$

where a' and b' are dimensionless parameters and oversonsolidation ratio is defined as $OCR_{p'} = \frac{p_o'(\zeta)}{p'}$. Based on Gallipoli et al. (2003), $p_o'(\zeta)$ is obtained from

$$\ln p_o'(\zeta) = \frac{\lambda - \kappa}{\frac{e}{e_s}(\zeta)\lambda - \kappa} \ln p_o'(0) + \frac{\left(\frac{e}{e_s}(\zeta) - 1\right) N}{\frac{e}{e_s}(\zeta)\lambda - \kappa} \tag{11}$$

in which

$$\frac{e}{e_s}(\zeta) = 1 - a[1 - \exp(b\zeta)] \tag{12}$$

where $\zeta = 1 - S_r$ and $e_s = N - \lambda \ln p'$. e_s is the saturated void ratio measured during virgin compression with respect to the same average soil skeleton stress corresponding to the

unsaturated void ratio, e. N is the intercept of the saturated normal compression line, λ is the slope of the saturated normal compression line and κ the saturated swelling index. $p_o^{'}(0)$ is the isotropic average soil skeleton stress on the saturated normal compression line. The function $h(S_r)$ is used to cater the effect of bonding due to water menisci. This model is more comprehensive than SEB2 and KM1 models as overconsolidation and bonding effects are explicitly considered.

KM2 model proposed a formulation to cater the effects of hydraulic hysteresis during drying-wetting cycle on shear modulus at very small strain. They adopted an effective degree of saturation instead of using degree of saturation for isotropic average skeleton stress (see Table 2). They used models by Wheeler et al. (2003) and Tamagnini (2004) in obtaining an expression for overconsolidation ratio by assuming the elastoplastic yield surface of the soil may change due to plastic deformation of soil or variation of matric suction. They decouple the effects of plastic compression and bonding due to water menisci and use two different exponent constants for those two effects. This model is similar to BMDJS model except void ratio function and function $h(S_r)$ is not included. For the second primary group, BMDJS was chosen to represent this group in the subsequent evaluation.

In the following, we evaluate the above mentioned models and propose a new simple formulation tackling the effects of stress and suction as well as collapse during wetting.

3. Proposed model for shear modulus of unsaturated soil at very small strain

Shear modulus at very small strain depends on current state of soil. In variably saturated soil, the state of soil may be described by net stress, matric suction, void ratio and degree of saturation. The following new formulation is suggested to predict the shear modulus at very small strain.

$$G_o = p_r A e^{-m} \left(\frac{p'}{p_r} \right)^n S_r^{-k/\lambda_p} \tag{13}$$

where p_r is a reference pressureof 1 kPa. A, n, m and k are model parameters controlling G_o magnitude and its dependency on mean effective stress, void ratio and degree of saturation.

The combined effect of net stress and matric suction is measured by means of effective stress. One of the possible formulations, which we adopt in the present work, is the stress from Equation 8, in which

$$\chi = S_r^{\gamma/\lambda_p} \tag{14}$$

where γ is taken as 0.55 following Khalili and Khabbaz (1998) and λ_p is the slope of water retention curve (WRC). Equation 14 is derived based on $\chi = \left(s_e s^{-1}\right)^{\gamma}$ from Khalili and Khabbaz (1998) and $S_r = \left(s_e s^{-1}\right)^{\lambda_p}$ from Brooks and Corey (1964), see D'Onza et al. (2011).

As a first approximation, the number of inter-particle contacts, which influence very small strain stiffness, may be measured by void ratio. For this reason, we adopt a function of void ratio in our formulation, instead of overconsolidation ratio.

The last term in the shear modulus expression quantify the bonding effect of water menisci at inter-particle contacts. We follow the approach by Trhlíková et al. (2012). They studied the effect of inter-particle bonding on shear modulus in cemented soils and found that it increases the very small strain shear modulus, additionally to the effect of effective mean stress. It is the number of water menisci, rather than the actual value of matric suction, which is controlling the water menisci bonding effect in partially saturated soils (Gallipoli et al., 2003) .The number of water menisci per unit volume of solid fraction is measured by degree of saturation, a function of which forms the last term in our G_o formulation.

The proposed model is summarised in Table 2 and evaluated together with other selected models.

4. Soils used for model calibration

Three different low plasticity fine grained soils, namely Zenoz kaolin, completely decomposed granite (CDT) and Po silt are used for evaluation of models. Zenoz kaolin as reported by Biglari et al. (2012) and Biglari et al. (2011) is a commercial Iranian kaolin. It is classified as CL according to the Unified Soil Classification System. Clay and silt fraction of Zenoz kaolin is about 18% and 60% respectively. CDT as reported by Ng and Yung (2008) and Ng et al. (2009) can be described as clayey silt (ML) according to the Unified Soil Classification System. The material is yellowish-brown, slightly plastic, with a very small percentage of fine and coarse sand. Po silt as reported by Vassallo et al. (2007a) is a clayey, slightly sandy silt. Based on Casagrande's chart, the material is classified as inorganic silt with low or high compresibility. Some of the properties for Zenoz kaolin, CDT and Po silt are summarised in Table 3.

5. Model calibration

Four models, namely NY, SEB1, BMDJS and the proposed models are evaluated in this study. For NY, SEB1, BMDJS and the proposed models, the variables are mean net stress, matric suction, void ratio and degree of saturation. For the proposed model, λ_p is also required. The effect of void ratio to λ_p is not considered in the evaluation presented in this paper as it does not have substantial effect on G_o. It is, however, pointed out that the variation of λ_p with void ratio proposed by Mašín (2010) will be used when incorporating the proposed G_o model into hypoplastic formulation. Variations of void ratio and degree of saturation with mean net stresses and suctions for Zenoz kaolin, CDT and Po silt are presented in Fig. 1 to 6. It should be noted variation of degree of saturation with mean net stresses for CDT is not available. The degree of saturation is inferred from water retention curve and does not vary with mean net stresses. The degree of saturation is respectively 1.0, 0.92, 0.77 and 0.65 for

suctions of 0, 50, 100 and 200 kPa. The calibration procedures for four models are described in this section.

5.1. Zenoz kaolin

The parameters A, m, n of NY and the proposed models are calibrated by fitting the shear modulus at very small strain from an isotropic loading-unloading test for a saturated soil. Parameter k of NY and the proposed models is obtained using shear modulus from an isotropic loading test at a suction of 50 kPa. Due to lack of geotechnical data, a constant λ_p of 0.18 is used for all the soil samples. This is obtained from WRC constructed using experimental data during wetting of an overconsolidated sample at mean net stress of 50 kPa as shown Fig. 7a. For SEB1 model, parameter n is taken as 0.5 as adopted in Sawangsuriya et al. (2009) and parameter A are obtained by fitting the shear modulus at very small strain from an isotropic loading test for a saturated soil. Parameter C of SEB1 model is obtained by fitting the shear modulus at very small strain from an isotropic loading test for an unsaturated soil at suction of 50 kPa. Parameters for BMDJS model are obtained from Biglari et al. (2011). Model parameters for NY, SEB1, BMDJS and proposed models are summarised in Table 4.

5.2. Completely decomposed tuff

For NY model, parameters A, m, n and k are obtained from Ng and Yung (2008). The parameters A and C for SEB1 model are determined based on the shear modulus at very small strain from isotropic loading tests at suctions of 0 and 100 kPa while parameter n is taken as 0.5. The parameters A, m, n and k for the proposed model are determined based on the shear modulus at very small strain from isotropic loading tests at suctions of 0, 50 and 100 kPa. λ_p for four suction-controlled isotropic compression tests performed at constant values of matric suction ranged from 0 to 200 kPa is taken as 0.25. For specimen tested at mean net stress of 110 kPa, the corresponding λ_p is estimated to be 0.84. This is obtained

from WRC constructed using experimental data during drying as shown in Fig.7b. For simplicity, λ_p during wetting is assumed to be 0.84. For specimen tested at mean net stress of 300 kPa, the corresponding λ_p is estimated to be 0.54 as shown in Fig.7b. For BMDJS model, parameters A and n are obtained by fitting the shear modulus at very small strain from isotropic loading tests for a saturated soil. The compressibility index, λ and intercept of normal compression line, N under saturated condition are obtained from compression curve in e:ln p' plane. As the liquid and plastic limits of CDT are similar to Po silt, the swelling index, κ is assumed to be the same as that measured for Po silt. Casagrande's graphical construction method is adopted in determination of the preconsolidation pressure using the compression curve in e:ln p' plane. The preconsolidation pressure for the soil specimens used for isotropic compression tests are 148, 245, 314 and 365 kPa respectively at suctions of 0, 50, 100 and 200 kPa. For drying-wetting tests, the compression curve for suction of 50 kPa is used to estimate the preconsolidation pressure since the after-compaction suction is 54 kPa. The fitting parameters for functions $e/e_s(\zeta)$ and $h(S_r)$ are determined following the procedures suggested by Biglari et al. (2011) using experimental data from isotropic loading tests at suctions of 100 and 200 kPa. Parameter m is obtained by fitting the shear modulus at very small strain from isotropic compression tests at suctions of 50 and 100 kPa. Model parameters for NY, SEB1, BMDJS and proposed models are summarised in Table 5.

5.3. Po silt

The parameters A, m, n and k for NY and the proposed models are determined by fitting the shear modulus at very small strain from an isotropic loading test at suction of 100 kPa and an isotropic loading-unloading test at suction of 200kPa. λ_p is estimated to be 0.11 as shown in Fig.7c. The parameters A and C for SEB1 model are determined based on the shear modulus at very small strain from isotropic loading tests at suctions of 100 and 200 kPa while parameter n is taken as 0.5. For BMDJS model, parameters N, λ and κ are also obtained from

compression curve in e:ln p' plane. Casagrande's graphical construction method is also adopted in determination of the preconsolidation pressure using the compression curve in e:ln p' plane. The preconsolidation pressure of the soil specimen used for isotropic compression test at suction of 100 kPa is 314 kPa. For isotropic loading-unloading-reloading test at suction of 100 kPa, the preconsolidation pressure of the soil specimen is 299 kPa. The preconsolidation pressures are 365 and 518 kPa respectively for soil specimens used for isotropic loading-unloading tests at suctions of 200 and 400 kPa. For drying test at mean net stress of 200 kPa, the corresponding compression curve at suction of 20 kPa is not sufficient to determine the preconsolidation pressure. The preconsolidation pressure of 122 kPa for a saturated specimen is adopted. Fitting parameters of functions $e/e_s(\zeta)$ are obtained by using measured void ratio and degree of saturation of soil specimens during isotropic loading tests at suctions of 100, 200 and 400 kPa. Fitting parameters of function $h(S_r)$ and parameters A and n are obtained by fitting the experimental data from isotropic loading tests at suction of 100 kPa and 200 kPa. Subsequently, parameter m is obtained by fitting shear modulus at very small strain from an isotropic unloading test at suction of 200 kPa. Model parameters for NY, SEB1, BMDJS and proposed models are summarised in Table 6.

6. Evaluation of models

6.1. Zenoz kaolin

Shear modulus at very small strain for commercial available Zenoz kaolin reported by Biglari et al. (2012) are used to evaluate the existing and proposed models in this section. The specimens were prepared using moist tamping method at a water content of about 11.9%, which was 3.5% dry of the optimum from standard Proctor compaction test. The adopted method was intended to prepare samples, which could be brought to a virgin state at

relatively low stress. The after-compaction suction was 240 kPa. Subsequently, the samples were brought up to mean net stress of 50 kPa.

Fig. 8 shows the shear modulus at very small strain during isotropic loading-unloading test for a saturated soil. As NY, BMDJS and proposed models are fitted to shear modulus during isotropic loading-unloading, the corresponding predictions agree well with the experimental data. Due to SEB1 model is calibrated using shear modulus during isotropic loading, thus a satisfactory prediction is expected. During isotropic unloading, SEB1 model underestimates the shear modulus. The predicted shear modulus during isotropic unloading is slightly larger than those during isotropic loading attributed to an increase in the value of void ratio function as the soil become denser after isotropic loading.

Fig. 9a compares predicted and measured shear modulus at very small strain during isotropic loading test at matric suction of 50 kPa. The specimen experiences plastic compression due to wetting-induced collapse when the after-compaction suction is reduced to 50 kPa. As all the models are fitted to the measured shear modulus, the corresponding predictions agree well with the experimental data. Fig. 9b compares predicted and measured shear modulus at very small strain at matric suction of 150 kPa. The specimen also experiences plastic compression due to wetting-induced collapse when the after-compaction suction is reduced to 150 kPa. All the models predict an increasing trend with mean net stress consistent with experimental data. BMDJS and proposed models give a good prediction on the shear modulus. NY model slightly underestimates but SEB1 model overestimates the shear modulus.

Fig. 10 shows the variations of shear modulus at very small strain during isotropic loading-unloading test at suction of 300 kPa. All the models predict a trend and amout of hysteresis consistent with the experimental data. It is found that SEB1 model overestimates the shear modulus the most, while the other models are closer to the data. The difference in predictions

are larger than those during isotropic loading at suction of 150 kPa as suction of 300 kPa is further from the suctions used in model calibrations.

Fig. 11a compares the predicted and measured shear modulus at very small strain during wetting for collapsible unsaturated soils. After equalization at mean net stress and matric suction of 50 and 300 kPa respectively, the mean net stress is increased to 350 kPa. Under a constant mean net stress of 350 kPa, the suction is reduced from 300 kPa to 50 kPa. All the models predict a decreasing trend when the suction is decreased from 300 to 50 kPa in contrast with the experimental data. For NY model, this suggests that the increase in shear modulus due to an increase in function ρe^m is unable to compensate the effect of suction reduction. For SEB1 model, this is because the increase in void ratio function does not compensate the reduction of shear modulus due to a decrease in function $S_r s$. For BMDJS model, this is because the increase in void ratio function does not compensate the reduction of shear modulus due to a decrease of average soil skeleton stress and function $h(S_r)$. For the proposed model, the increase in predicted shear modulus attributed to the increase in void ratio function is less than the decrease due to reduction of average skeleton stress and bonding effect. BMDJS model gives the best prediction among the models. When suction is reduced from 300 kPa to 150 kPa, the predictions by the proposed model is similar to those by the comprehensive BMDJS model.

Fig. 11b compares the predicted and measured shear modulus at very small strain during wetting for non-collapsible unsaturated soils. After equalization at mean net stress and matric suction of 50 and 300 kPa respectively, the mean net stress is increased to 250 kPa and reduced to 50 kPa subsequently. Under a constant mean net stress of 50 kPa, the suction is reduced from 300 kPa to 50 kPa. NY model predicts reduction in shear modulus as suction reduces from 300 to 50 kPa, slight increase as suction increases from 50 to 70 kPa and reduction as suction reduces from 70 to 25 kPa. This trend is consistent with the experimental

data. The trends predicted by SEB1, BMDJS and the proposed models are also consistent with the experimental data.

6.2. Completely decomposed tuff

In this section, shear modulus at very small strain for completely decomposed tuff (CDT) as reported by Ng and Yung (2008), Ng et al. (2009) and Yung (2004) are used in the evaluation. The measured matric suction after sample preparation was about 54 kPa.

Fig. 12 shows the shear modulus at very small strain during isotropic loading tests at suction of 0 to 200 kPa. Each of the specimens used in the isotropic compression tests had initial mean net stress of 110 kPa after an equalisation stage. The degree of saturation is assumed to be constant during the isotropic loading. Fig. 12a shows the shear modulus for a saturated specimen. Shear modulus predicted by all the models agree well with the experimental data. This is not suprising as the test is used to calibrate the models. Fig. 12b to 12d compares the measured and predicted shear modulus at suction of 50 to 200 kPa. All the models give an increasing trend consistent with the experimental data and predictions agrees well with the data. The discrepancy increase as suctions increases, as tests at low suctions are used for model calibration.

Fig. 13 shows the variations of shear modulus at very small strain with suction during first drying-wetting cycle at mean net stress of 110 and 300 kPa. After compaction, the mean net stresses of the soil specimens are increased to 110 and 300 kPa respectively while the suction was reduced to zero for equalisation.The matric suction was increased from zero to 250 kPa during drying path and reduced to zero when the wetting path was completed. At the same suction and mean net stress, the shear modulus predicted by NY and SEB1 models during wetting are consistently lower than those predicted during drying. This trend is contradictory with experimental data. Degree of saturation on wetting path is smaller than that on drying path as shown in Fig. 4b. Thus, the bulk density in NY model at wetting path is smaller than

that at wetting path at the same suction. For NY model, the effect of bulk density on shear modulus does not compensate by the effect due to change of void ratio. For SEB1 model, the contradictory trend is due to the function S_rs at wetting path is smaller than that at drying path.

Both BMDJS and the proposed model predict a trend consistent with the experimental data. But the predicted shear modulus hysteresis is insignificant as compared to the experimental data. The proposed model leads to correct prediction because the average soil skeleton stress at wetting path is smaller than that at drying path while the bonding effects at wetting path are larger than that at drying path. These contradictory effects result in the predicted shear modulus at wetting path is larger than that at drying path.

6.3. Po silt

Shear modulus at very small strain for Po silt as reported by Vassallo et al. (2007a) are used in the evaluation in this section. The soil was compacted at the optimum water content as shown in Table 3. The after-compaction suction was inferred to be about 140 kPa. Each of the specimens had initial mean net stress of 10 kPa after an equalisation stage.

Fig. 14a compared the predicted and measured shear modulus at very small strain during isotropic loading test at suction 100 kPa. All the models give good predictions of shear modulus as the experimental data is used to calibrate the models. Fig. 14b compares the predicted and measured shear modulus during isotropic loading-unloading-reloading test at suction of 100 kPa. Though the predicted hysteresis by NY and the proposed models during isotropic unloading-reloading is small, both models predict a trend consistent with the experimental data. Shear modulus predicted by SEB1 and BMDJS models agree well with experimental data during isotropic loading but both models underestimate the shear modulus during isotropic unloading and reloading though the predicted trends are consistent with the experimental data.

Fig. 15a shows the shear modulus at very small strain during isotropic loading-unloading test at matric suction of 200 kPa. NY, BMDJS and the proposed models give reasonably good prediction during isotropic loading and unloading as the experimental data is used to calibrate the models. As SEB1 model is fitted to the measured shear modulus during isotropic loading, the corresponding prediction agrees well with the experimental data. However, SEB1 model underestimates the shear modulus during isotropic unloading. Fig 15b shows the shear modulus at very small strain during isotropic loading-unloading test at matric suction of 400 kPa. During isotropic loading, NY model gives a good prediction. Both SEB1 and BMDJS models overestimate the shear modulus while the proposed model underestimates it. During isotropic unloading, all the models underestimate the shear modulus. NY, BMDJS and the proposed model predict a hysteresis though it is smaller than the experimental data. Contrary, the predicted hysteresis by SEB1 model is negligible.

Fig. 16 shows the shear modulus at very small strain during drying at net stress of 200 kPa. After equalization at mean net stress of 10 kPa and matric suction of 20 kPa, the mean net stress was increased to 200 kPa. Subsequently, the suction was increased to 400 kPa at constant mean net stress of 200 kPa. All the models predict an increasing trend consistent with the experimental data. Shear modulus predicted by NY model is in good agreement with experimental data for suction up to 200 kPa but underestimates the experimental data for suction at 400 kPa. SEB1, BMDJS and proposed models underestimate the shear modulus.

Fig. 17 compares the predicted and measured shear modulus at small strain during drying and wetting cycles at mean net stress of 200 kPa. After equalization at mean net stress of 10 kPa and matric suction of 200 kPa, the mean net stress was increased to 200 kPa. Subsequently, the suction was increased to 400 kPa and reduced to 100 kPa twice. Finally, the suction is increased to 200 kPa.

Fig. 17a compares the shear modulus predicted by NY and SEB1 models with experimental data. NY and SEB1 models predict a significant increase in shear modulus as suction is first increased from 200 to 400 kPa consistent with the experimental data. During wetting-drying cycles, the predicted shear modulus by NY and SEB1 models at suction of 100 kPa and 400 kPa are almost constant while the measured value is slightly increased. For NY model, the predicted shear modulus at the end of the wetting-drying cycles at suction of 200 kPa is larger than that at the beginning of the cycles consistent with the experimental data. This is attributed to the function e^m at the end of cycles is larger than that at the beginning of the cycles due to a decrease in void ratio at the end of the cycles as the change of S_r is relatively insignificant. In contrast, the predicted shear modulus by SEB1 model at the end of the wetting-drying cycles at suction of 200 kPa is almost identical to that at the beginning of the wetting-drying cycles. The adopted void ratio function changes insignificantly with the reduction of void ratio at the end of the cycles.

Fig. 17b shows the variations of shear modulus with suction for BMDJS and the proposed models. Both BMDJS and the proposed models also predict a significant increase in shear modulus as suction is first increased from 200 to 400 kPa. For BMDJS model, the predicted shear modulus at suction of 100 kPa and 400 kPa are increased with number of wetting-drying cycle. The increase is mainly attributed to function $h(S_r)$ due to a small decrease in the degree of saturation as the number of wetting-drying cycle increases. The predicted shear modulus by the proposed model at suction of 100 kPa and 400 kPa are almost constant during the wetting-drying cycles. For BMDJS and the proposed model, the predicted shear modulus at the end of the wetting-drying cycles at suction of 200 kPa is larger than that at the beginning of the wetting-drying cycles. The BMDJS model gives the best prediction in this case.

Fig. 18 shows the shear modulus at very small strain during wetting and drying cycles at mean net stress of 200 kPa. After equalization at mean net stress of 10 kPa and matric suction of 400 kPa, the mean net stress was increased to 200 kPa. Subsequently, the suction reduced to 100 kPa and increased to 400 kPa. Then, the suction was reduced to 100 kPa. Apart from SEB1 model, all the models predicts cyclic increase of shear modulus. This agrees with the experimental data trend, although the amount of modulus increase is under-predicted. In addition, the SEB1 model under-predicts shear modulus at suction of 100 kPa and BMDJS model over-predicts shear modulus at suction of 400 kPa.

7. Summary and conclusions

A new model has been proposed in this study for predicting shear modulus at very small strain. There is a clear physical reasoning for the structure of the newly proposed model. Several selected models from literature, namely NY model proposed by Ng and Yung (2008), SEB1 model suggested by Sawangsuriya et al. (2009), BMDJS model presented by Biglari et al. (2011) and the newly proposed model have subsequently been evaluated. Shear modulus at very small strains for three different low plasticity fine grained soils available in the literature are used in the evaluation.

It is found that the NY, BMDJS and the newly proposed models can predict shear modulus at very small strains in low plasticity fine grained soil resulting from an increase and a decrease of mean net stress at a constant suction. Moreover, BMDJS and the proposed models are able to give a reasonably good prediction on shear stiffness at very small strain during wetting of a collapsible unsaturated soil. It is found that BMDJS model gives the best prediction among the models during wetting of a collapsible unsaturated soil. Both BMDJS and the proposed models can predict a consistent trend with measured shear stiffness at very small strains of non-collapsible soils during drying-wetting cycles. In contrast, both SEB1 and NY models may give an inconsistent trend.

This evaluation revealed that the newly proposed model has better predictive capabilities than some earlier formulations of the same simplicity such as NY and SEB1 models. In addition, the proposed model has similar predictive capability as an earlier formulation which is more complex to calibrate. This is useful in practical design of geotechnical structures especially when there is lack of experimental data to calibrate a complex model.

Acknowledgements

Financial support by the research grant GACR P105/12/1705 is greatly appreciated. The first author has been supported by a post-doc grant at Charles University in Prague.

References

Alonso, E. E., Gens, A., and Josa, A. (1990). "A constitutive model for partially saturated soils." Geotechnique, 40(3), 405-430.

Biglari, M., d'Onofrio, A., Mancuso, C., Jafari, M. K., Shafiee, A., and Ashayeri, I. (2012). "Small-strain stiffness of Zenoz kaolin in unsaturated conditions." Canadian Geotechnical Journal, 49(3), 311-322.

Biglari, M., Mancuso, C., d'Onofrio, A., Jafari, M. K., and Shafiee, A. (2011). "Modelling the initial shear stiffness of unsaturated soils as a function of the coupled effects of the void ratio and the degree of saturation." Computers and Geotechnics, 38(5), 709-720.

Brooks, R., and Corey, A. (1964). "Hydraulic properties of porous media." Hydrology paper No. 3, Colorado state University.

D'Onza, F., Gallipoli, D., Wheeler, S., Casini, F., Vaunat, J., Khalili, N., Laloui, L., Mancuso, C., Mašín, D., Nuth, M., Pereira, J. M., and Vassallo, R. (2011). "Benchmark of constitutive models for unsaturated soils." Géotechnique, 61(4), 283-302.

Gallipoli, D., Gens, A., Sharma, R., and Vaunat, J. (2003). "An elasto-plastic model for unsaturated soil incorporating the effects of suction and degree of saturation on mechanical behaviour." Geotechnique, 53(1), 123-135.

Kayadelen, C., Tekinsoy, M. A., and Taskiran, T. (2007). "Influence of matrix suction on shear strength behavior of a residual soil." Environmental Geology, 53(4), 891-901.

Khalili, N., and Khabbaz, M. H. (1998). "A unique relationship for Ï‡ for the determination of the shear strength of unsaturated soils." Geotechnique, 48(5), 681-687.

Khosravi, A., and McCartney, J. S. (2009). "Impact of stress state on the dynamic shear moduli of unsaturated, compacted soils." 4th Asia-Pacific Conference on Unsaturated Soils.

Khosravi, A., and McCartney, J. S. (2012). "Impact of hydraulic hysteresis on the small strain shear modulus of low plasticity soils." Journal of Geotechnical and Geoenvironmental Engineering, 138(11), 1326-1333.

Leong, E. C., Cahyadi, J., and Rahardjo, H. (2006) "Stiffness of a compacted residual soil." Geotechnical Special Publication, 1168-1180.

Lu, N., and Likos, W. J. (2006). "Suction stress characteristic curve for unsaturated soil." Journal of Geotechnical and Geoenvironmental Engineering, 132(2), 131-142.
Mancuso, C., Vassallo, R., and D'Onofrio, A. (2002). "Small strain behavior of a silty sand in controlled-suction resonant column - Torsional shear tests." Canadian Geotechnical Journal, 39(1), 22-31.
Mašín, D. (2010). "Predicting the dependency of a degree of saturation on void ratio and suction using effective stress principle for unsaturated soils." International Journal for Numerical and Analytical Methods in Geomechanics, 34(1), 73-90.
Mašín, D. (2013). "Clay hypoplasticity with explicitly defined asymptotic states." Acta Geotechnica, 8(5), 481-496.
Mašín, D., and Khalili, N. (2008). "A hypoplastic model for mechanical response of unsaturated soils." International Journal for Numerical and Analytical Methods in Geomechanics, 32(15), 1903-1926.
Mašín, D., and Rott, J. (2013). "Small strain stiffness anisotropy of natural sedimentary clays: review and a model." Acta Geotechnica, In print, corrected proof.
Ng, C. W. W., and Xu, J. (2012). "Effects of current suction ratio and recent suction history on small-strain behaviour of an unsaturated soil." Canadian Geotechnical Journal, 49(2), 226-243.
Ng, C. W. W., Xu, J., and Yung, S. Y. (2009). "Effects of wetting-drying and stress ratio on anisotropic stiffness of an unsaturated soil at very small strains." Canadian Geotechnical Journal, 46(9), 1062-1076.
Ng, C. W. W., and Yung, S. Y. (2008). "Determination of the anisotropic shear stiffness of an unsaturated decomposed soil." Geotechnique, 58(1), 23-35.
Sawangsuriya, A., Edil, T. B., and Bosscher, P. J. (2009). "Modulus-suction-moisture relationship for compacted soils in postcompaction state." Journal of Geotechnical and Geoenvironmental Engineering, 135(10), 1390-1403.
Tamagnini, R. (2004). "An extended Cam-clay model for unsaturated soils with hydraulic hysteresis." Geotechnique, 54(3), 223-228.
Trhlíková, J., Mašín, D., and Boháč, J. (2012). "Small strain behaviour of cemented soils." Géotechnique, 62(10), 943-947.
Vassallo, R., Mancuso, C., and Vinale, F. (2007a). "Effects of net stress and suction history on the small strain stiffness of a compacted clayey silt." Canadian Geotechnical Journal, 44(4), 447-462.
Vassallo, R., Mancuso, C., and Vinale, F. (2007b). "Modelling the influence of stress-strain history on the initial shear stiffness of an unsaturated compacted silt." Canadian Geotechnical Journal, 44(4), 463-472.
Wheeler, S. J., Sharma, R. S., and Buisson, M. S. R. (2003). "Coupling of hydraulic hysteresis and stress-strain behaviour in unsaturated soils." Geotechnique, 53(1), 41-54.
Yung, S. Y. (2004). "Determination of shear wave velocity and anisotropic shear modulus of unsaturated soil," MPhil thesis, Hong Kong University of Science and Technology.

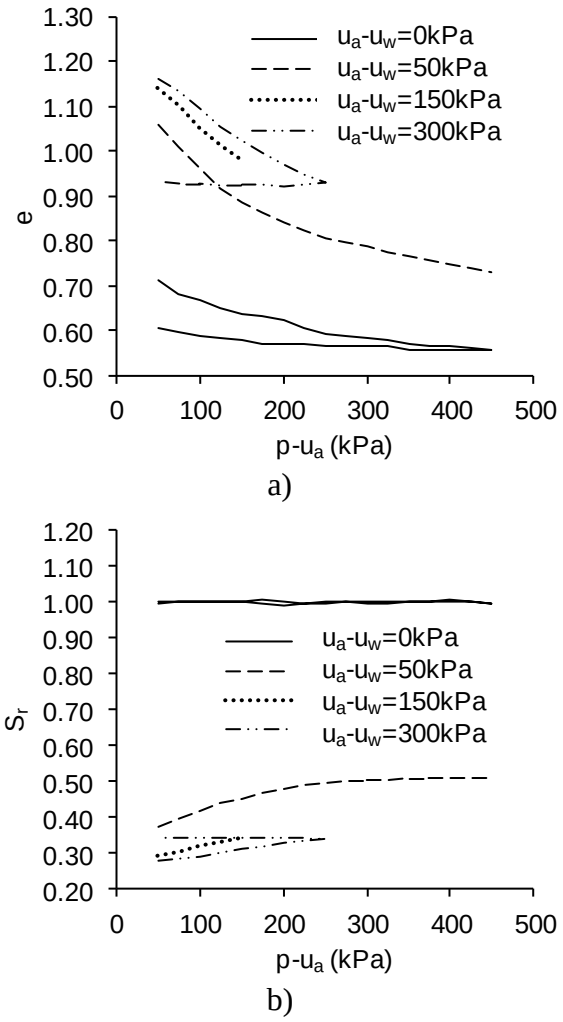

Fig. 1. Variations of a) void ratio; b) degree of saturation with net mean stress for Zenoz kaolin

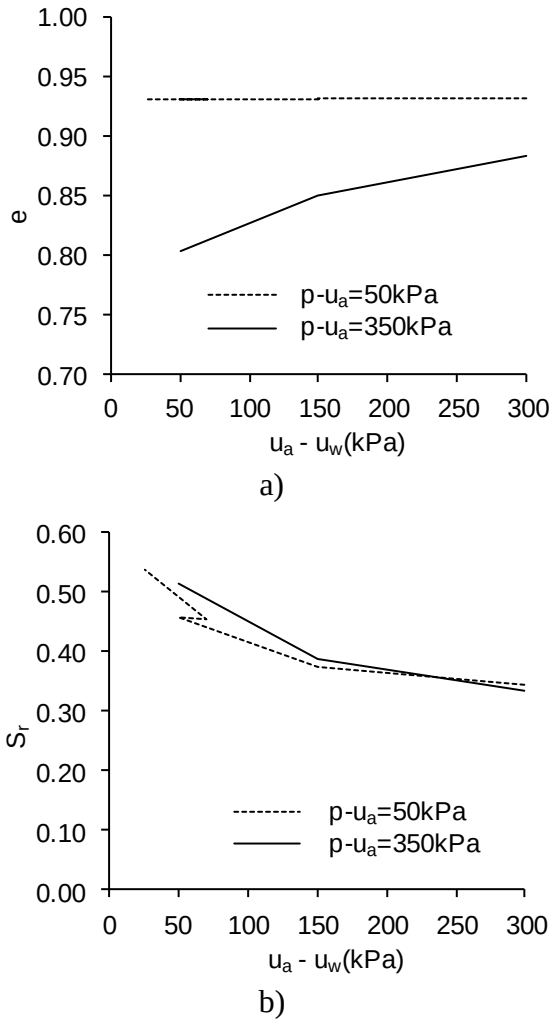

Fig. 2. Variations of a) void ratio; b) degree of saturation with suction for Zenoz kaolin

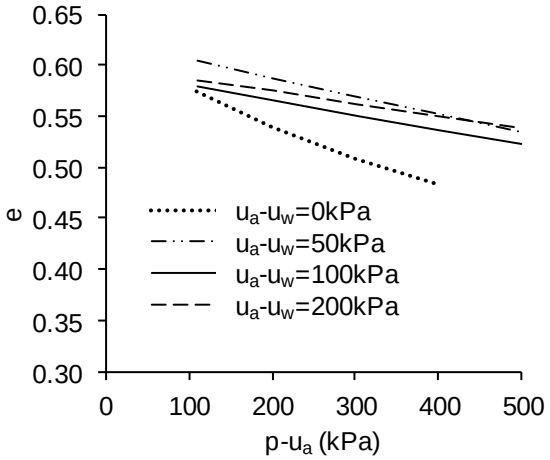

Fig. 3. Variations of void ratio with net mean stress for CDT

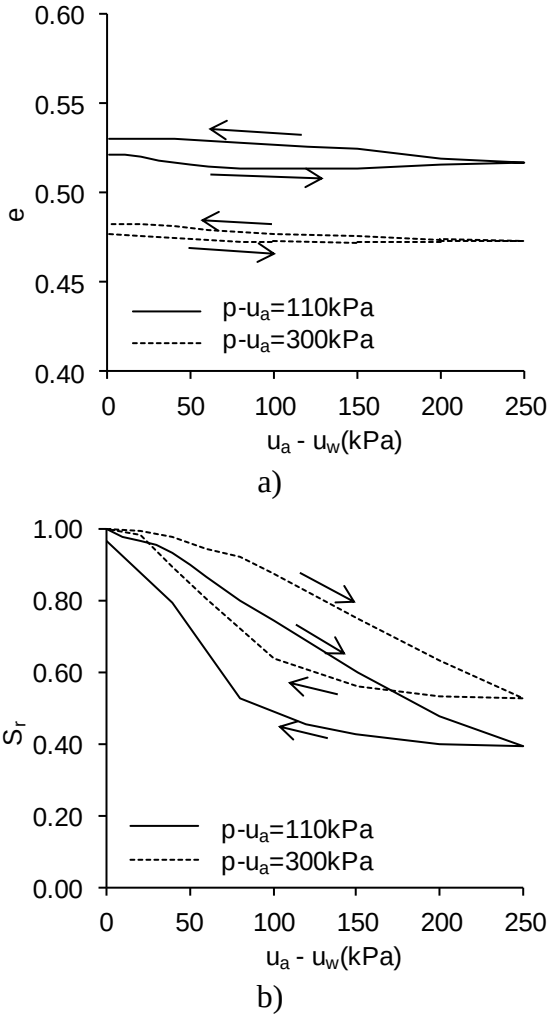

Fig. 4. Variations of a) void ratio; b) degree of saturation with suction for CDT

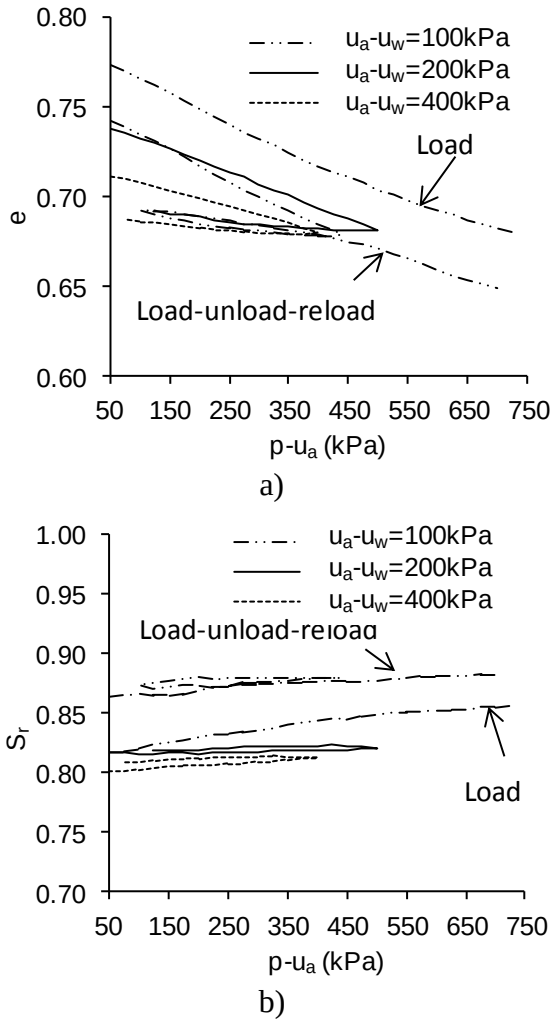

Fig. 5. Variations of a) void ratio; b) degree of saturation with net mean stress for Po silt

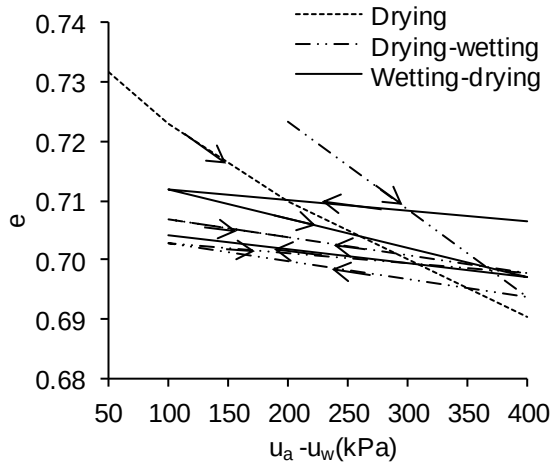

a)

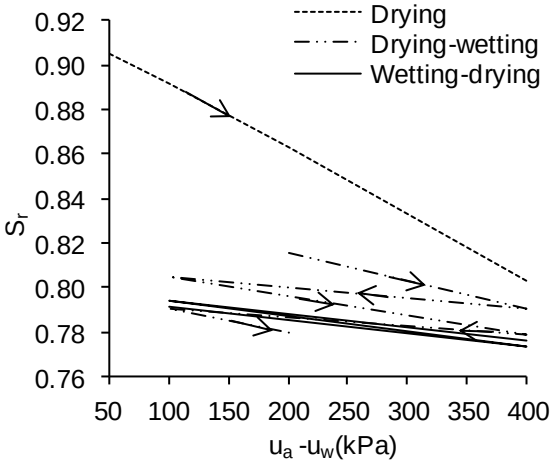

b)

Fig. 6. Variations of a) void ratio; b) degree of saturation with suction for Po silt

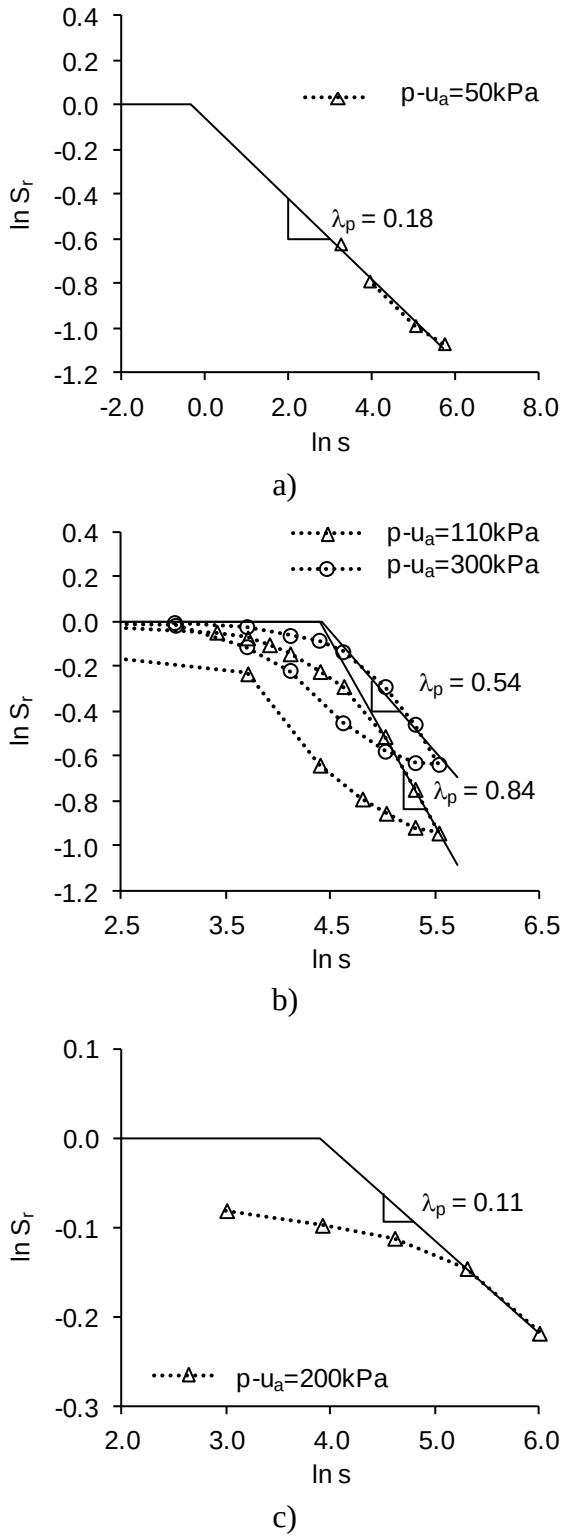

Fig. 7. Soil water characteristic curves for: a) Zenoz kaolin; b) CDT; c) Po silt

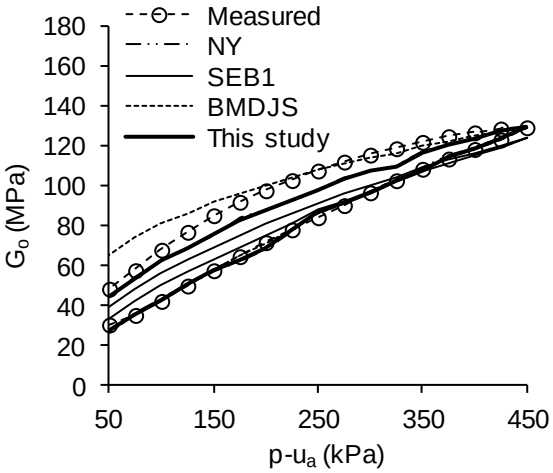

Fig. 8. Prediction of shear modulus at very small strain during an isotropic loading-unloading test for saturated Zenoz kaolin

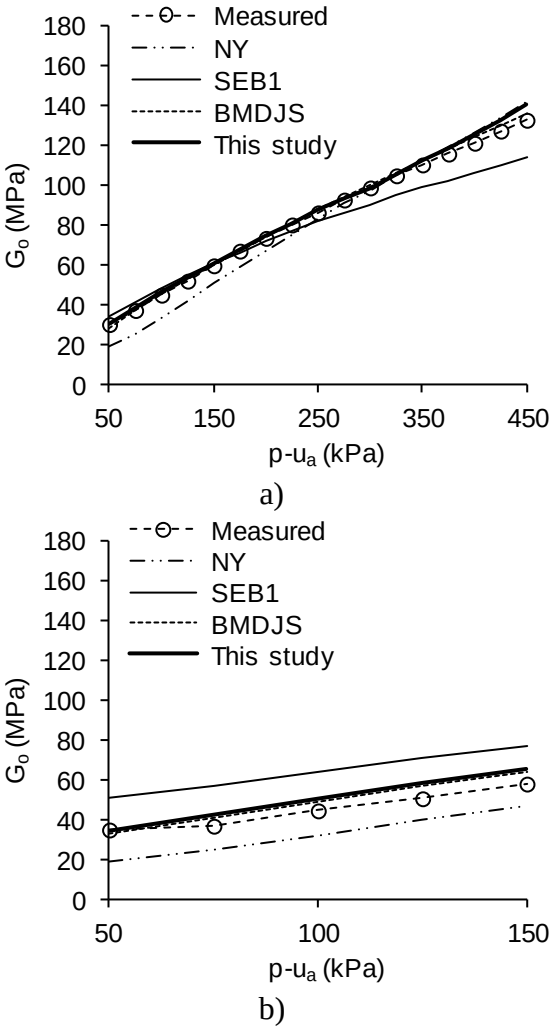

Fig. 9. Prediction of shear modulus at very small strain for unsaturated Zenoz kaolin during isotropic loading tests at suctions of: a) 50 kPa; b) 150 kPa

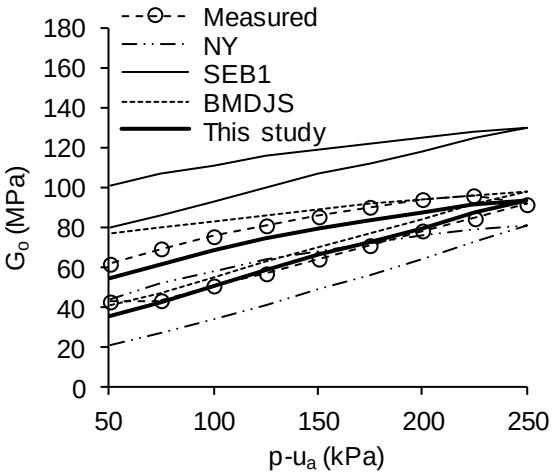

Fig. 10. Prediction of shear modulus at very small strain during an isotropic loading-unloading test for unsaturated Zenoz kaolin at suction of 300 kPa

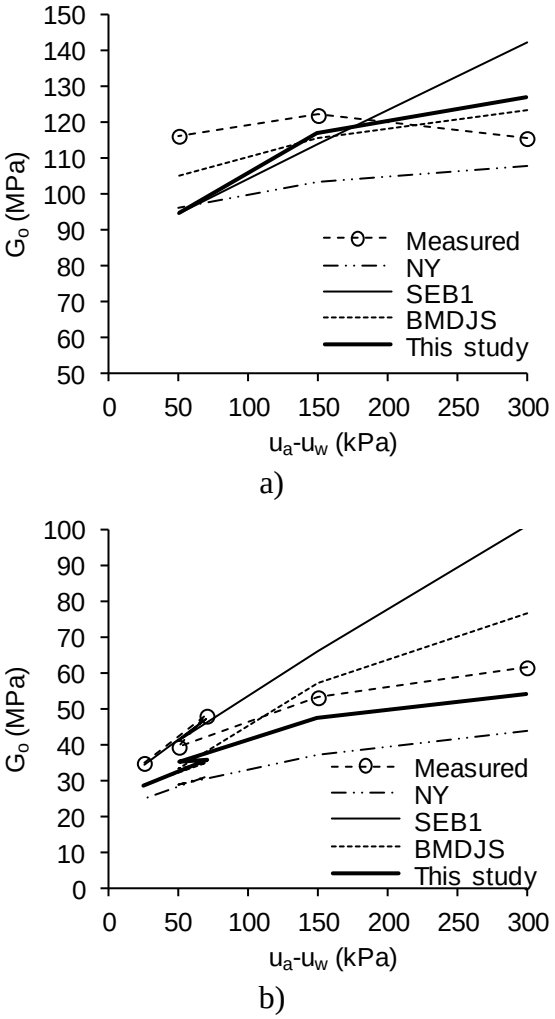

Fig. 11. Prediction of shear modulus at very small strain during wetting for a) normal consolidated; b） overconsolidated unsaturated Zenoz kaolin

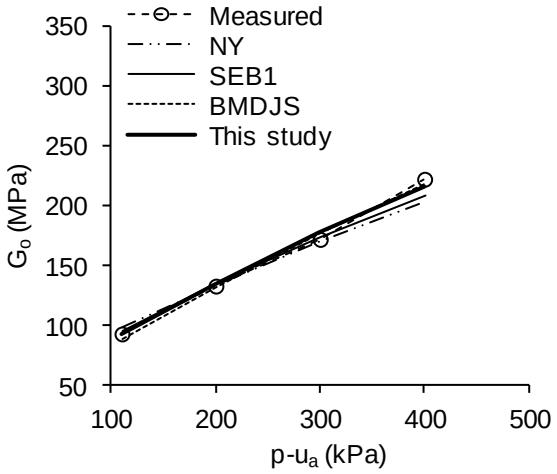
Measured
NY
SEB1
BMDJS
This study
350
300
250
200
150
100
50
G_o (MPa)
100
200
300
400
500
p-u_a (kPa)

a)

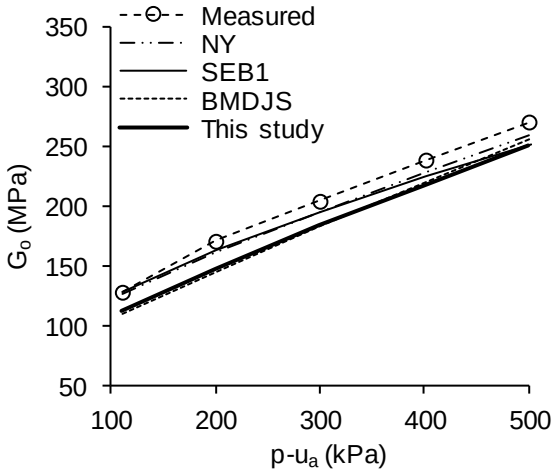
Measured
NY
SEB1
BMDJS
This study
350
300
250
200
150
100
50
G_o (MPa)
100
200
300
400
500
p-u_a (kPa)

b)

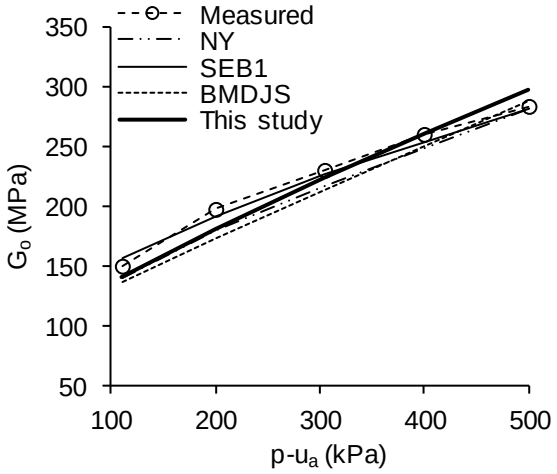
Measured
NY
SEB1
BMDJS
This study
350
300
250
200
150
100
50
G_o (MPa)
100
200
300
400
500
p-u_a (kPa)

c)

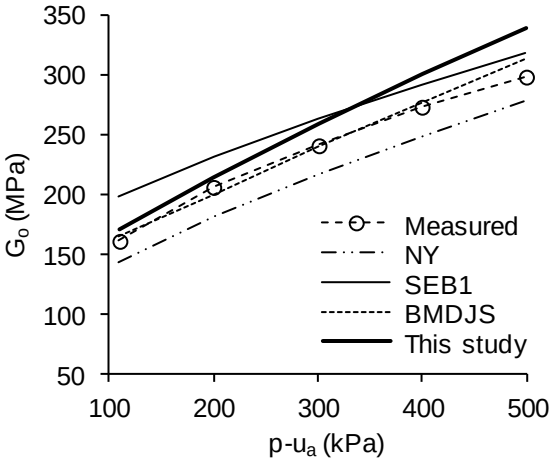

d)

Fig. 12. Prediction of shear modulus at very small strain during isotropic loading tests for unsaturated CDT at mean net stresses of: a) 0 kPa; b) 50 kPa; c) 100 kPa; d) 200 kPa

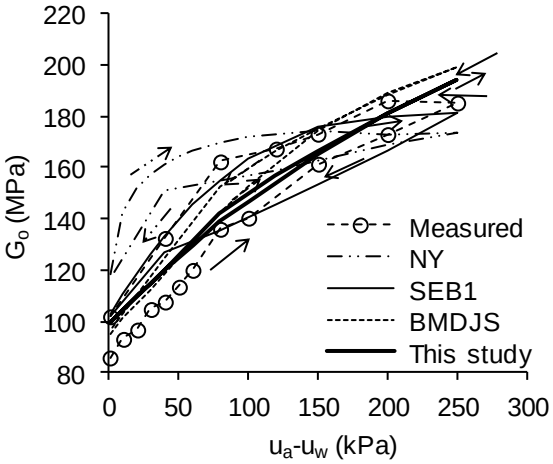

a)

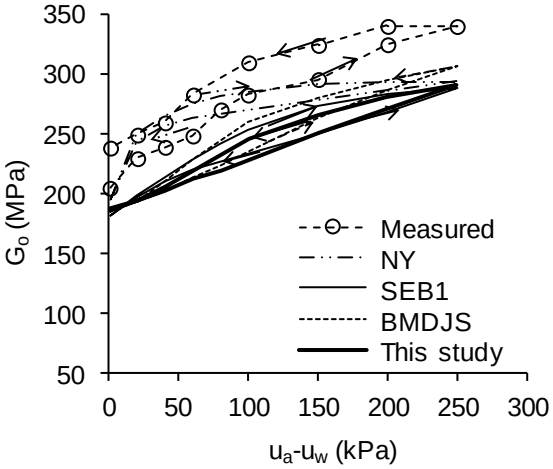

b)

Fig. 13. Prediction of shear modulus at very small strain during drying-wetting cycle for unsaturated CDT at mean net stresses of : a) 110 kPa; b) 300 kPa

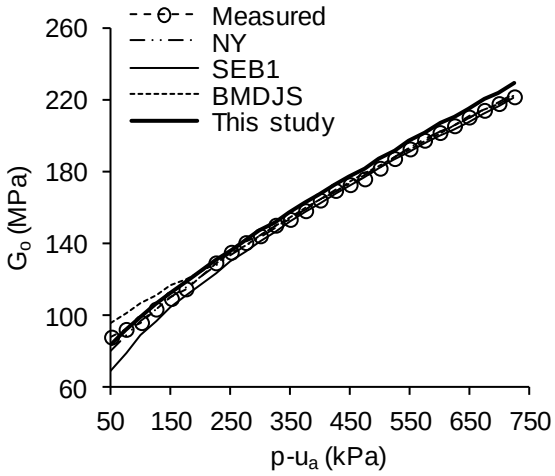

a)

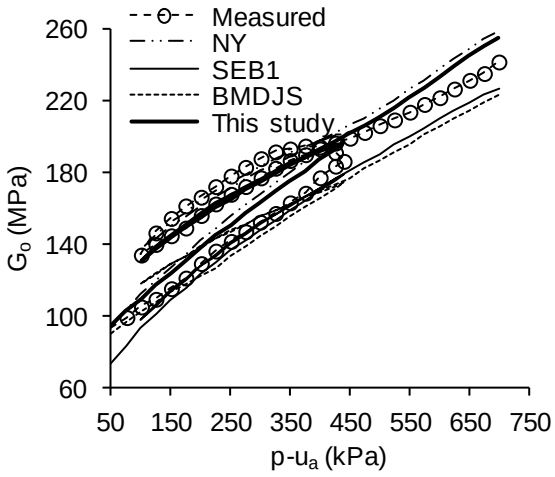

b)

Fig. 14. Prediction of shear modulus at very small strain during isotropic a) loading; b) loading-unloading-reloading tests for unsaturated Po silt at suction of 100 kPa

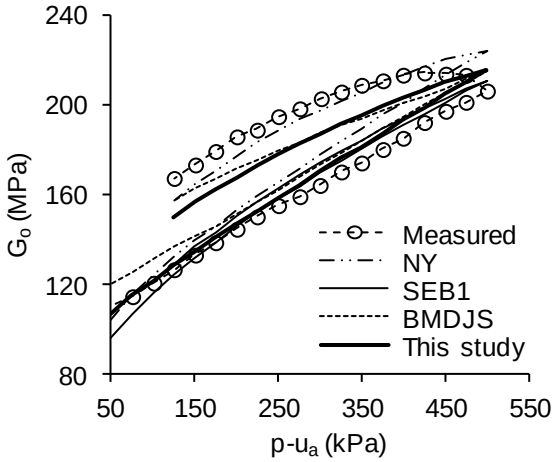

a)

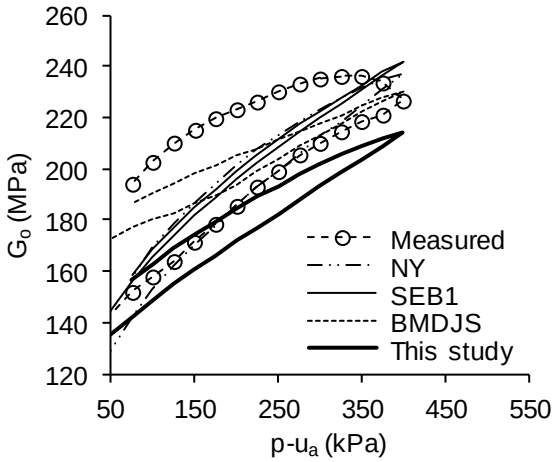

b)

Fig. 15. Prediction of shear modulus at very small strain during isotropic loading-unloading tests for Po silt at suctions of a) 200 kPa; b) 400 kPa

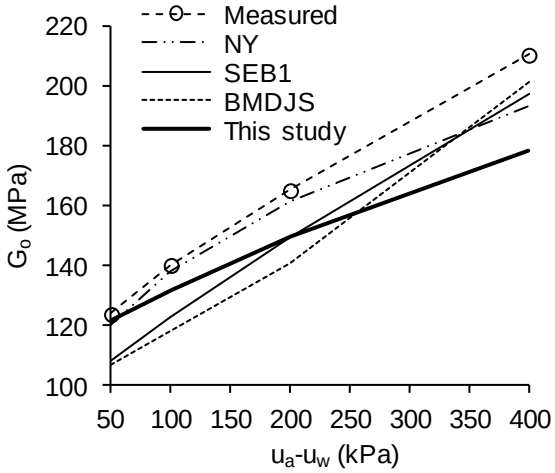

Fig. 16. Prediction of shear modulus at very small strain during drying for Po silt at mean net stress of 200 kPa

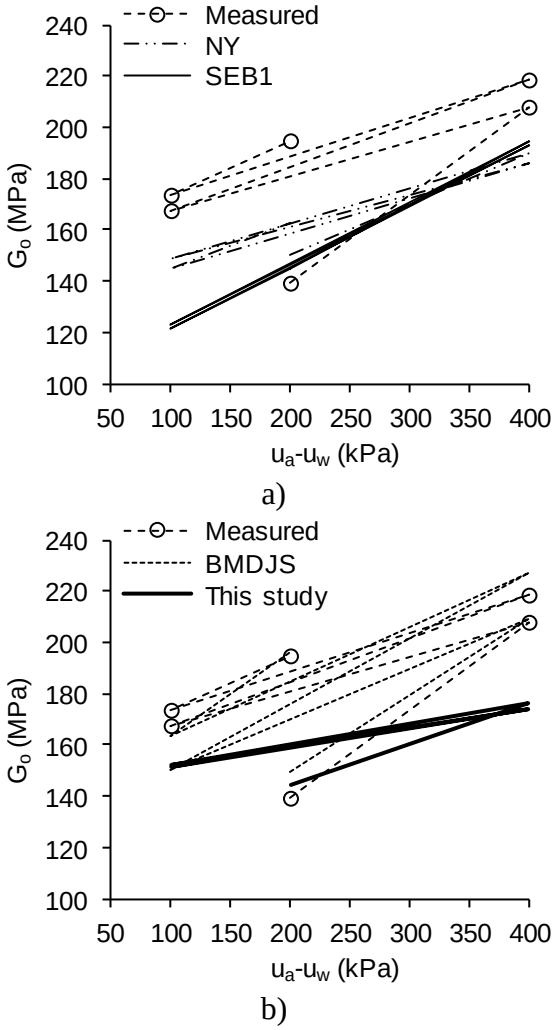

Fig. 17. Prediction of shear modulus at very small strain during drying-wetting cycles for unsaturated Po silt at mean net stress of 200 kPa using: a) NY and SEB1 models; b) BMDJS and new models

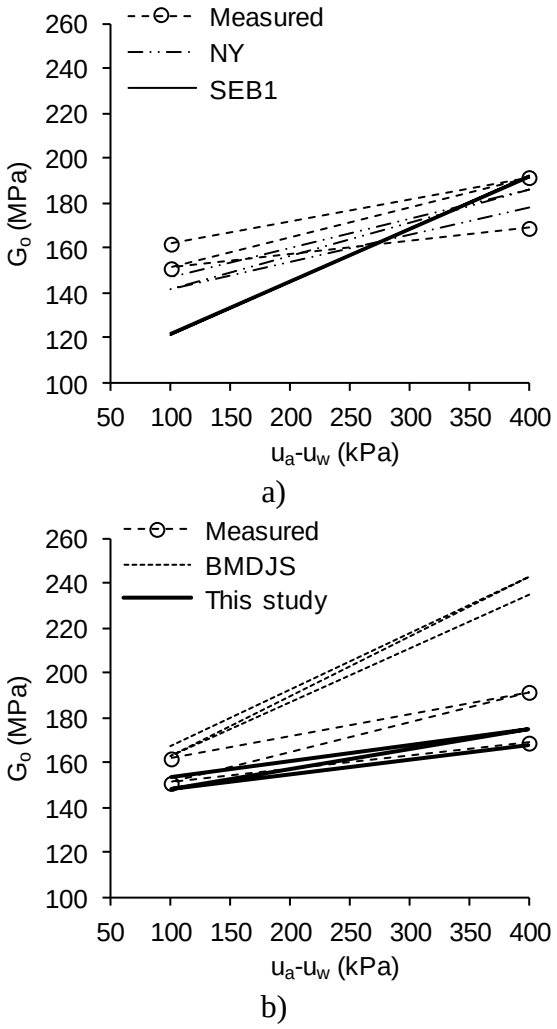

Fig. 18. Prediction of shear modulus at very small strain during wetting-drying cycles for unsaturated Po silt at mean net stress of 200 kPa using: a) NY and SEB1 models; b) BMDJS and new models

Table 1 Models for shear modulus at very small strain with general form of $G_o = \alpha f(p-u_a)g_1(s)+\beta g_2(s)$

No	Model	α	$f(p-u_a)$	$g_1(s)$	β	$g_2(s)$	Adopted in evaluation
1	Mancuso, Vassallo & d'Onofrio (MVD)	$Ap_a^{1-n}OCR^m$	For $s < s_e$, $[(p-u_a)+s]^n$ For $s > s_e$, $[(p-u_a)+s_e]^n$	For $s < s_e$, 1 For $s > s_e$, $h(s)$	0	-	No
2	Leong, Cahyadi & Rahardjo (LCR)	A	$1+[(p-u_a)/p_a]^n$	$1+[\ln(1+s/p_a)]^k$	0	-	No
3	Ng & Yung (NY)	$A\rho e^m$	$[(p-u_a)/p_r]^n$	$(1+s/p_a)^k$	0	-	Yes
4	Vassallo, Mancuso & Vinale (VMV)	$Ap_af_1(e)OCR^mH(s_o/s)$	$[(p-u_a)/p_a]^n$	-	$p_af_1(e)$	?	No
5	Sawangsuriya, Edil & Bosscher first (SEB1)	$Af_2(e)$	$(p-u_a)^n$	-	CS_r^{Θ}	s	Yes

Notes:-

1. $f_1(e) = (2.973-e)^2/(1+e)$
2. $f_2(e) = 1/(0.3+0.7e^2)$
3. $H(s_o/s) = (1-r)\exp\{-\beta[s_o/s -1]\}+r$
4. $h(s) =[1-r_s]\exp[-\beta_s(s-s_e)]+r_s$
5. $OCR = (p-u_a)_o/(p-u_a)$
6. $\Theta = 1$

Table 2 Models for shear modulus at very small strain with general form of $G_o = \alpha f(p-u_a,s)$

No	Model	α	$f(p-u_a,s)$	Adopted in evaluation
1	Sawangsuriya, Edil & Bosscher second (SEB2)	$Af_2(e)$	$[(p-u_a)+ S_r^{\Theta}s]^n$	No
2	Khosravi & McCartney (KM1)	$Ap_a^n f_2(e)$	$[(p-u_a)/p_a+(1+s_e/p_a)\ln(1+s/p_a)]^n$	No
3	Biglari, Mancuso, d'Onofrio, Jafari & Shafiee (BMDJS)	$Ap_a^{1-n} f_1(e) OCR_p^m$	$[(p-u_a)+S_r s]^n\, h(S_r)$	Yes
4	Khosravi & McCartney (KM2)	$Ap_a^{1-n} OCR_{p'}^m$	$[(p-u_a)+S_e s]^n$	No
5	This study	$Ap_r^{1-n} e^{-m}$	$[(p-u_a)+ S_r^{\gamma/\lambda p}s]^n S_r^{-k/\lambda p}$	Yes

Notes:-

1. $f_1(e) = (2.973-e)^2/(1+e)$
2. $f_2(e) = 1/(0.3+0.7e^2)$
3. For BMDJS model, $OCR_{p'} = \dfrac{p_o'(\zeta)}{p'}$; $h(S_r) = 1-a'\left[1-\exp\left(b'\zeta\right)\right]$; $\zeta = 1-S_r$
4. For KM2 model, $OCR_{p'}^m = \left(\dfrac{p_c'}{p'}\right)^m = \left[\dfrac{p_{co}'}{(p-u_a)}\exp\left(\dfrac{\Delta e^p}{\lambda-\kappa}\right)\right]^K \left[\dfrac{(p-u_a)}{p'}\exp\left(b\left[S_{eo}-S_e\right]\right)\right]^{K'}$; p_c' is the mean yield stress; Δe^p is an increment of void ratio along the virgin compression line; $S_e = (S_r - S_{res})/(1-S_{res})$ where S_{res} is degree of consolidation at residual saturation condition. S_{eo} and p_{co}' are the initial values of S_e and p_c'; K, K' and b are dimensionless parameters
5. In this study, $\chi = (s_e/s)^{0.55}$
6. $\Theta = 1$

Table 3 Index properties of soils used in the evaluation of models

Parameter	Zenoz kaolin	CDT	Po silt
Maximum dry density: kN/m^3	17.4	17.3	15.5
Optimum water content: %	15.4	16.3	23.1
Percentage of sand: %	22	24	33
Percentage of silt: %	60	72	40
Percentage of clay: %	18	4	27
Specific gravity	2.65	2.73	2.74*
Liquid limit: %	29	43	51*
Plastic limit: %	17	29	33*
Plasticity index: %	12	14	18*
Classification(USCS)	CL	ML	ML/MH

*average value of four samples

Table 4 Model parameter values used by models for Zenoz kaolin

Parameter	NY model	SEB1 model	BMDJS model	This study
A	1150.21	3000	134.32	2176.12
m	-2.81	-	0.345	3.05
n	0.380	0.5	0.626	0.375
k	0.260	-	-	0.243
C	-	750	-	-
N	-	-	0.997	-
λ	-	-	0.0725	-
κ	-	-	0.02	-
a	-	-	0.104	-
b	-	-	2.91	-
a'	-	-	0.143	-
b'	-	-	2.355	-
λ_p	-	-	-	0.18

* assumed value

Table 5 Model parameter values used by models for CDT

Parameter	NY model	SEB1 model	BMDJS model	This study
A	3994.24	4800	221.41	4216.67
m	-1.54	-	0.05	0.90
n	0.340	0.5	0.620	0.548
k	0.09	-	-	0.20
C	-	800	-	-
N	-	-	0.978	-
λ	-	-	0.083	-
κ	-	-	0.015*	-
a	-	-	1.90	-
b	-	-	0.30	-
a'	-	-	2.40	-
b'	-	-	0.20	-
λ_p	-	-	-	varies

* assumed value

Table 6 Model parameter values used by models for Po silt

Parameter	NY model	SEB1 model	BMDJS model	This study
A	4085.10	4500	226.67	8686.28
m	-3.00	-	0.15	3.00
n	0.222	0.5	0.520	0.297
k	0.15	-	-	0.09
C	-	300	-	-
N	-	-	1.026	-
λ	-	-	0.065	-
κ	-	-	0.015	-
a	-	-	0.01	-
b	-	-	10	-
a'	-	-	0.0015	-
b'	-	-	25	-
λ_p	-	-	-	0.11

* assumed value